PALEOCEANOGRAPHY, VOL. 14, NO. 2, PAGES 224-231, APRIL 1999

High-resolution U^K_{37} temperature reconstructions in the South China Sea over the past 220 kyr

Carles Pelejero and Joan O. Grimalt
Department of Environmental Chemistry (CID-CSIC), Barcelona, Catalonia, Spain

Stephanie Heilig,[1] Markus Kienast,[1] and Luejiang Wang[2]
Institut fuer Geowissenschaften, University of Kiel, Kiel, Germany

Abstract. Past sea surface temperatures (SST) in the northern and southern areas of the South China Sea have been reconstructed for the past 220 kyr using the U^K_{37} alkenone index. The SST profiles follow the glacial/interglacial pattern exhibiting differences between Last Glacial Maximum and Holocene that are 1°-3°C larger than those observed at the same latitudes in the Atlantic and Pacific Oceans. In Termination I both planktonic foraminiferal $\delta^{18}O$ and SST exhibit well-defined Bølling-Allerød and Younger Dryas events with temperature differences between both periods of 0.8° and 0.4°C in north and south, respectively. SSTs record a constant north-south difference of 1°C in the interglacials and nearly 2.5°C in the glacial stages. These differences define two distinct climatic and water circulation patterns that correspond with glacial/interglacial sea level oscillations which opened and closed water exchange with the tropical Indo-Pacific Ocean through the present Sunda Shelf.

1. Introduction

The South China Sea (SCS) is the largest marginal basin in the western Pacific and lies under the influence of the Western Pacific Warm Pool, an area with important feedback to the Asian monsoon system [*Wang and Wang*, 1990; *Miao et al.*, 1994]. Its location between the east Asian land mass and the western Pacific makes this marginal sea very sensitive to climate changes in both land and sea. The SCS is also strongly affected, over glacial/interglacial timescales, by sea level changes. This is because the SCS has broad shelves in the northwest and southwest which emerged during low sea level stands, diminishing the contact to the open Pacific in the north and completely closing the channels to the tropical Indo-Pacific waters in the south [*Broecker et al.*, 1988; *Wang and Wang*, 1990].

In the SCS, sedimentation rates are particularly high during interglacials and even higher during glacial times, primarily because of the emergence of vast land areas together with the numerous river discharges [*Schönfeld and Kudrass*, 1993; *Wang et al.*, 1998]. This affords a chance to carry out high-resolution paleoceanographic studies.

The present work is devoted to the study of past sea surface temperatures (SST) in the SCS by means of the C_{37}-alkenone-derived U^K_{37} index paleothermometer. SST reconstructions in the SCS have already been addressed in several previous studies, mainly by means of foraminiferal transfer functions [*Wang and Wang*, 1990, and references therein]. The newly developed U^K_{37} index technique has only recently been applied in the north of the SCS over the past 25 kyr [*Huang et al.*, 1997a, b].

The U^K_{37} index has been successfully used for reconstructing SST changes over the latest climatic cycle in a variety of locations, in the Atlantic [e.g., *Brassell et al.*, 1986; *Zhao et al.*, 1993; *Madureira et al.*, 1995; *Summerhayes et al.*, 1995; *Villanueva et al.*, 1998], the Indian [e.g., *Rostek et al.*, 1993; *Bard et al.*, 1997], and the Pacific Oceans [e.g., *McCaffrey et al.*, 1990; *Prahl et al.*, 1993]. The method provides a robust temperature proxy for paleoclimatic studies and is free from bias originating from the partial dissolution of calcareous tests [*Sikes et al.*, 1991], which often alter SST estimates on the basis of the faunal abundance of planktonic foraminifera [*Berger*, 1968; *Miao et al.*, 1994]. Sedimentary C_{37} alkenone ratios provide good SST estimates in warm environments, such as the SCS, where high water production is reflected in high abundances of C_{37} alkenones [*Pelejero and Grimalt*, 1997].

The present study is based on four deep-sea cores of undisturbed hemipelagic sediments from the northern and southern SCS (Figure 1 and Table 1) [*Sarnthein et al.*, 1994]. The sites selected provide a representative data set for the SCS under the influence of the tropical Indo-Pacific and/or Pacific Ocean surface waters. At present the former enters through the Malaca, Gaspar, and Karimata Straits and flows across the Sunda Shelf during summer following a northeastward direction; the latter enters through the Bashi and Taiwan Straits during winter, following a southwest direction.

2. Materials and Methods

The four cores considered in this study (Figure 1 and Table 1) were obtained during R/V Sonne cruise in April-June 1994 [*Sarnthein et al.*, 1994]. They were collected at roughly the same water depth range of 1520 - 1968 m.

Core profile 17940 (Figure 2) comprises a composite of a gravity core and a box core. The composite stratigraphy is based on high-resolution foraminiferal $\delta^{18}O$ and $\delta^{13}C$ determinations with the surface of the gravity core corresponding to 2.5 cm in the box core [*Wang et al.*, 1998]. Core profile 17964 (Figure 2) consists of a composite of a gravity and a piston core and foraminiferal $\delta^{18}O$,

[1]Now at Department of Geoscience, University of British Columbia, Vancouver, British Columbia, Canada.
[2]Now at Department of Geoscience, Graduate School of Environmental Earth Science, Hokkaido University, Sapporo, Japan.

Paper number 1998PA900015.
0883-8305/99/1998PA900015$12.00

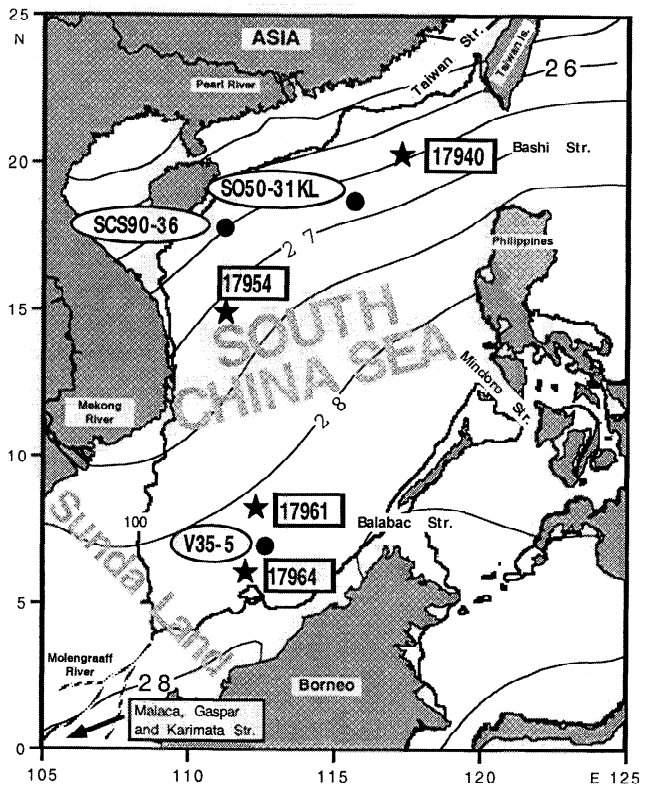

Figure 1. Map of the South China Sea showing the location of the studied cores (stars) collected during the R/V Sonne cruise in April-June 1994 [*Sarnthein et al.*, 1994]. The locations of other cores discussed in the text are also indicated (solid circles): SO50-31KL and SCS90-36 [*Huang et al.*, 1997a, b] and V35-5 [*Broecker et al.*, 1988]. The inferred course of the Molengraaff River during glacial times is shown according to*Molengraaff* [1921]. The 100 m isobath (thick dark line) approximately represents the coastline during glacial times. Thin dark isolines correspond to modern annual average temperatures (degrees Celsius) at 0 - 30 m depth [*Levitus*, 1994].

$\delta^{13}C$, and $CaCO_3$ % curves indicating a downward shift of 200 cm in the piston core relative to the gravity core [*Kienast*, 1996; *Jian et al.*, 1998].

The stratigraphy of all records is based on accelerator mass spectrometry (AMS)-^{14}C datings and on planktonic (*Globigerinoides ruber*) and benthic (*Cibicidoides wuellerstorfi*) foraminiferal $\delta^{18}O$ records (*Wang et al.* [1998] and unpublished benthic foraminifera data of core 17954). The age control points for each core are shown in Figure 2. The age model of core 17940 for 0-11.6 ka is based on a smooth spline fit across the age-depth control points, where ^{14}C ages are converted to calendar ages. For ages older than the Preboreal (>11,600 calendar years (cal. years) B.P.), the chronostratigraphy of core 17940 was established by tuning the light $\delta^{18}O$ peaks in stages 2-3 to the warm Dansgaard-Oeschger events 2-10 in the $\delta^{18}O$ record of the annual resolution ice core Greenland Ice Sheet Project (GISP) 2 [*Grootes and Stuiver*, 1997]. Details of this age model are given by *Wang et al.*, [1998]. In cores 17961 and 17964 the end of the Last Glacial Maximum (LGM) was defined as the heaviest value in the benthic foraminiferal $\delta^{18}O$ record. An age of 17.2 cal kyr was assigned to it by analogy with the AMS-^{14}C dated 17940 core.

Samples were selected at 1-20 cm intervals depending on the sedimentation rate at the stations and the period studied. The most detailed reconstruction is from core 17940, with a time resolution at least bidecadal in the Holocene. The lowest resolution is reported at sites 17961 and 17954, particularly in the oldest parts of the records, with time intervals of 5 kyr per sample.

The procedures and equipment used for U^K_{37} index determinations are described elsewhere [*Villanueva et al.*, 1997]. Briefly, sediment samples were freeze-dried and manually ground for homogeneity. After the addition of an internal standard (a mixture of *n*-nonadecan-1-ol, *n*-hexatriacontane, and *n*-tetracontane), dry subsamples (~ 3 g) were extracted with dichloromethane in an ultrasonic bath. The extracts were hydrolyzed with 6% potassium hydroxide in methanol to eliminate interferences from wax esters. The hexane extracts were then fractionated by silica column chromatography to separate hydrocarbons and ketones from the polar fraction. After bis(trimethylsilyl)trifluoroacetamide derivatization the extracts were analyzed by gas chromatography with flame ionization detection. Selected samples were examined by gas chromatography-mass spectrometry for confirmation of compound identification and evaluation of possible coelutions. The amounts of alkenones found in all samples ranged between 130 and 2300 ng g dry sediment (Table 2). Replication of a sediment sample with similar lipid content and U^K_{37} index five times showed a standard deviation of ±0.15°C in temperature estimation.

3. Results

3.1. Calibration Equation

To date most studies of U^K_{37}-derived paleotemperatures have used the equations of *Prahl and Wakeham* [1987] (U^K_{37} = 0.033SST + 0.043) or *Prahl et al.* [1989] (U^K_{37} = 0.034SST + 0.039) for the transformation of sedimentary U^K_{37} values into paleo-SSTs. Both equations were calibrated using cultures of *Emiliania huxleyi* at different growth temperatures.

In the SCS, calibration of U^K_{37} in sediment core tops *versus* SST from *Levitus* [1994] data showed a good linear relationship (R = 0.926) for annually averaged 0- 30 m SST, resulting in the equation U^K_{37} = 0.031SST + 0.092 [*Pelejero and Grimalt*, 1997]. A global core-top calibration using U^K_{37} data from 370 sites in the Atlantic, Indian, and Pacific Oceans and modern surface (0 m) annual mean temperatures recently yielded the equation U^K_{37} = 0.033SST + 0.044 [*Müller et al*, 1998], and since it is the most extensive compilation, using all core-top data available to date, it has been recommended for future paleotemperature reconstructions.

Temperatures obtained with both equations for the four SCS core tops are compared in Table 2 with the modern annual mean temperatures at 0-30 m and 0 m water depth [*Levitus*, 1994]. This shows that the SCS equation is more appropriate since it matches the 0 - 30 m depth temperatures with differences of only 0.1°-0.2°C for cores 17954, 17961, and 17964 and of 0.5°C for core 17940. In contrast, the global core-top calibration by *Müller et al.* [1998], which should indicate 0 m depth temperatures, shows temperatures that are systematically higher by 0.7°C for 17954,

Table 1. Locations and Water Depths of the South China Sea (SCS) Cores Considered in This Study

Core	Latitude, N	Longitude, E	Depth, m
17940	20°7.0'	117°23.0'	1727
17954	14°47.8'	111°31.5'	1520
17961	8°30.4'	112°19.9'	1968
17964	6°9.5'	112°12.8'	1556

Further details are given by *Sarnthein et al.* [1994].

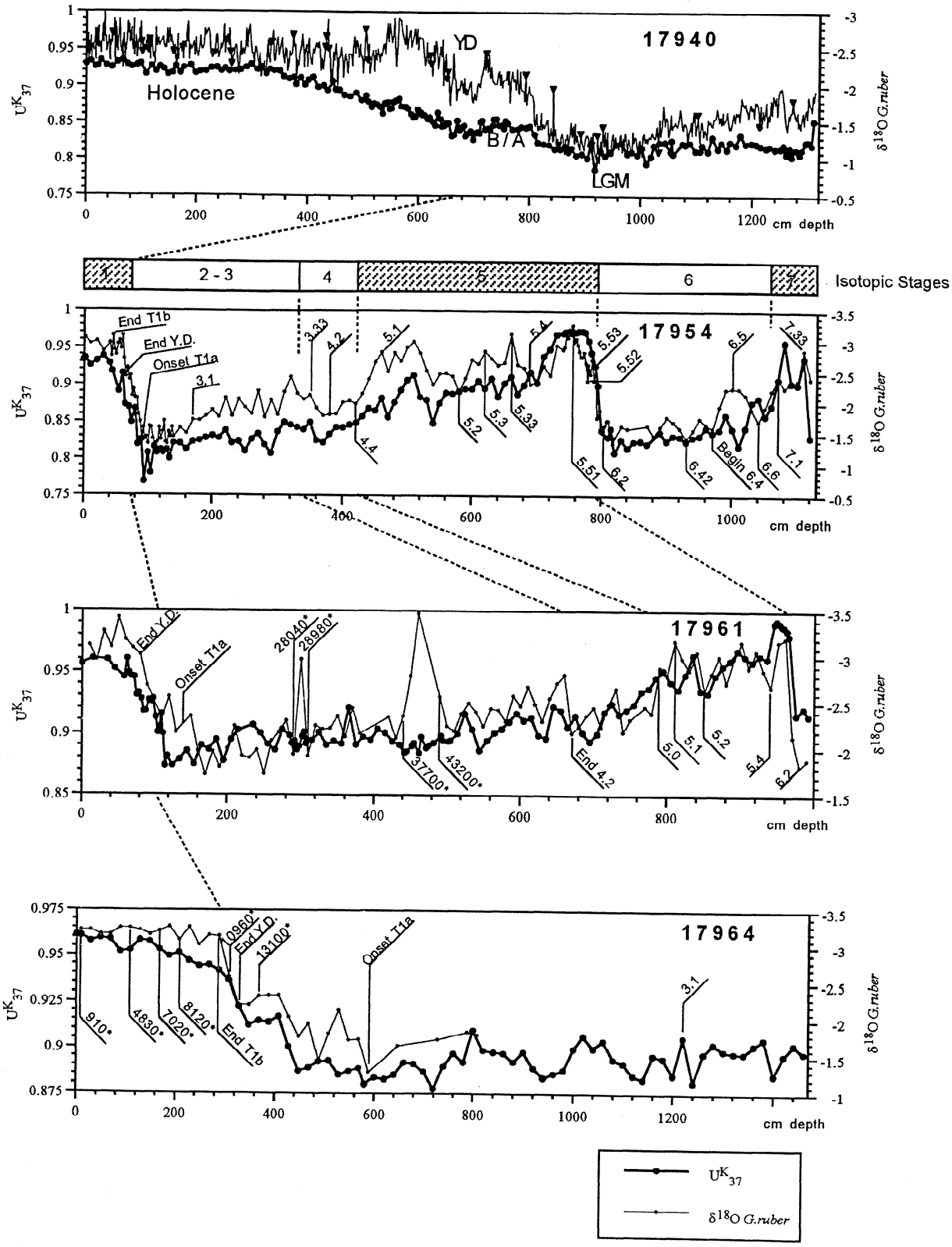

Figure 2. U^{K}_{37} index (thick line) and planktonic foraminifera *Globigerinoides ruber* $\delta^{18}O$ (thin line) depth profiles of the cores studied in this work. The age points in each core are indicated (see details by *Wang et al.* [1998]). Values in cores 17961 and 17964 marked with an asterisk correspond to calibrated years (Accelerator mass spectrometry (AMS)-^{14}C were corrected by 400 years reservoir age according to *Bard et al.* [1990b] and converted to calendar years according to *Stuiver and Braziunas*, [1993] and *Bard et al.* [1990a]). Marine oxygen isotopic stages are labeled according to *Martinson et al.* [1987]. In core 17940 a total of 40 AMS-^{14}C dates were obtained (marked with solid triangles). Exact ages and details on the age model are given by *Wang et al.* [1998].

Table 2. Comparison of U^{K}_{37} - Temperatures Obtained With the SCS Equation With Those Obtained With the Global Core-Top Calibration

Core	Modern SST 0 - 30 m, °C	U^{K}_{37} SST,[a] °C	modern SST 0 m, °C	U^{K}_{37} SST,[b] °C	C_{37} alkenones, ng g
17940	26.5	27.0	26.8	26.8	600-1800
17954	27.2	27.1	27.6	26.9	200-2300
17961	28.0	27.8	28.3	27.6	260-1500
17964	28.2	28.0	28.5	27.8	130-1100

Modern temperatures for each location at 0-30 m depth and at 0 m depth are also shown [*Levitus*, 1994]. Note the better agreement with the use of the SCS equation.

[a]SCS equation $U^{K}_{37} = 0.031SST + 0.092$ [*Pelejero and Grimalt*, 1997], corresponding to the 0 - 30 m annual average temperature.

[b]Global core-top equation: $U^{K}_{37} = 0.033SST + 0.044$ [*Müller et al.*, 1998], corresponding to the 0 m annual average temperature.

17961, and 17964, although it matches the 17940 temperature. In view of these results the use of the SCS equation seems more appropriate for the SCS reconstructions presented in this paper.

3.2. SST Variations Over the Past 220 kyr

U^{K}_{37} profiles and $\delta^{18}O$ of the planktonic foraminifera *G. ruber* [*Wang et al.*, 1998] are shown in Figure 3. Although the four cores have similar lengths (10-14 m), the age periods covered in each case are very different because of the large differences in sedimentation rate. The northernmost and the southernmost cores, 17940 and 17964, respectively, approximately reach down to midstage 3 (sedimentation rates of 20-85 and 30-55 cm kyr^{-1}, respectively). In contrast, core 17961 reaches the end of stage 6, and core 17954 has the maximum age coverage of 220 ka (6-9 and 3-10 cm kyr^{-1}, respectively).

The high sedimentation rates in cores 17940 and 17964 are mainly due to riverine influences. Core 17940 is situated ~400 km off the Pearl River mouth (Figure 1), the second largest modern water discharge of China. Core 17964 was collected at a site under the influence of the Molengraaff River, a drainage system which appeared in the southwest SCS during glacial times [*Molengraaff*, 1921] when sea level was lower than at present [Fairbanks, 1989].

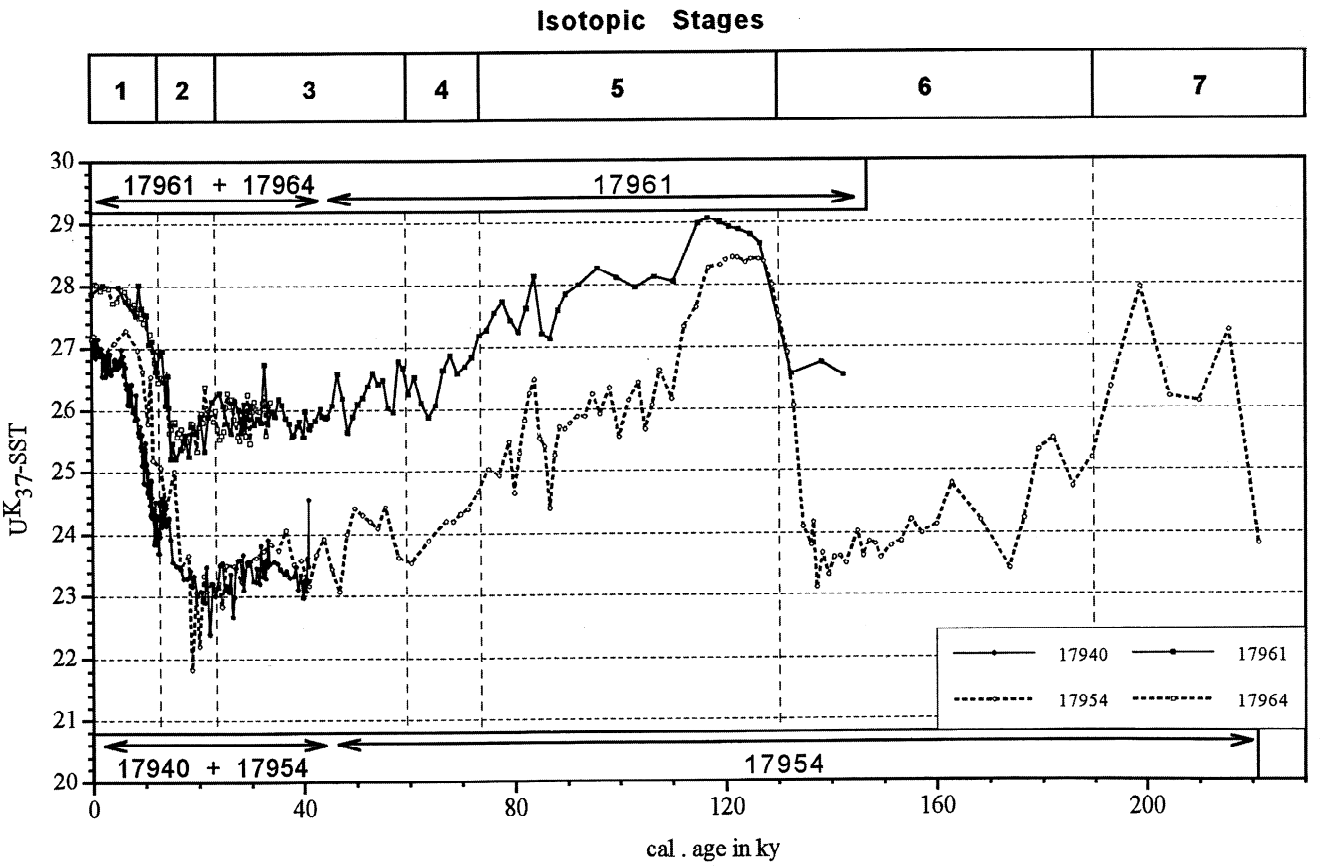

Figure 3. U^{K}_{37}-sea surface temperature (SST) reconstruction of the four SCS cores studied. The two upper curves correspond to the southern cores, 17961 and 17964. The two lower curves correspond to the northern core, 17940, and the northwestern core, 17954. SSTs were estimated using the SCS equation $U^{K}_{37} = 0.031SST + 0.092$ [*Pelejero and Grimalt*, 1997] and represent annual average temperatures at 0-30 m depth.

The other two cores, 17954 and 17961, are much farther away from major riverine influence.

As a general trend, the U^{K}_{37} signal follows a glacial/interglacial pattern in all four stations, paralleling the *G. ruber* $\delta^{18}O$ profile (Figure 2). As shown in Figure 3, the SST values obtained using the SCS equation [*Pelejero and Grimalt*, 1997] for the two northernmost stations, 17940 and 17954, oscillate between the same absolute SST values. The same is true for the southernmost cores 17964 and 17961, which display about the same SST values throughout the records.

Following the records from the oldest to the youngest interval, warm stage 7, which is only recorded in core 17954 (Figure 3), has a derived SST of 28°C, an intermediate temperature between the Holocene and stage 5e. Although this result is obtained with low resolution sampling, the same temperature differences have been observed in a recent U^{K}_{37}-SST reconstruction for the North Atlantic [*Villanueva et al.*, 1998].

Stage 6 shows 1°-1.4°C warmer temperatures than stage 2 (cores 17954 and 17961; Figure 3). The same feature has been observed in the North Atlantic [*Villanueva et al.*, 1998]. During stage 6 the temperatures of these two SCS records are offset by 3°C, a difference that is larger than the north-south gradient observed during stage 2, 2.2°C.

Stage 5e (Eemian, cores 17954 and 17961; Figure 3) shows 1°-1.2°C warmer temperatures than the Holocene. This pattern has also been observed in the South Atlantic Ocean [*Schneider et al.*, 1995] and the Mediterranean Sea [*Cornu et al.*, 1993].

Temperatures during stage 5e were remarkably stable, increasing smoothly from 28.6° to 29°C in the south (17961) and remaining almost constant at 28.4°C in the north (17954). Thus it appears that the SCS was quite stable in terms of SST in stage 5e, with the north-south gradient increasing smoothly through time. This SST stability contrasts with the *G. ruber* $\delta^{18}O$ record during this warm stage, particularly in core 17954, which shows significant changes: -2.5 to –3.2‰ and back to former values (Figure 2). Thus the isotopic changes can be interpreted to reflect global ice volume or salinity changes. The abrupt *G. ruber* $\delta^{18}O$ changes in this core are also observed in the Sulu Sea [*Linsley*, 1996], which, in turn, are well correlated with sea level variations derived from the Huon Peninsula coral terraces [*Chappell and Shackleton*, 1986]. In this respect the Younger Dryas type signal for Termination II identified by *Linsley* [1996] also seems to be recorded in 17954 (Figure 2)[*Heilig*, 1996].

Moving forward in time, comparison of cores 17961 and 17954 (Figure 3) shows that SSTs followed the same trend in the northern and southern SCS through the last glacial cycle, with a progressive cooling from 28.4° to 23.4°C in the north (17954) and from 29° to 25.2°C in the south (17961), culminating at the LGM. The strong parallelism in the SST records between the northern and southern cores also involves specific events such as a warming period centered at 85 ka B.P., preceded and followed by two cooling events (87 and 80 ka). This signal is recorded as 2° and 1°C temperature maxima in the north and south, respectively.

Temperature differences between the south (17961 and 17964) and the north (17940 and 17954) show two distinct climatic patterns, one involving a south-north average difference of 2-2.5°C and the other involving an average difference of only 0-1°C. These two patterns roughly correspond to the glacial and interglacial periods, with lower SST differences between the north and south during interglacials. Transitions from one pattern to the other seem to have occurred over short time periods. Thus, at the end of stage 5e, 112 - 110 kyr B.P., there is a well-defined SST decrease of 1.2°C in core 17954 (north) which is not recorded in core 17961 (south). Later, during the warming from LGM to Holocene conditions the temperature difference between the south and north decreases again.

These clear shifts in climatic patterns at the 5e/5d boundary and at Termination I could be indicators of drastic changes in low-latitude Pacific and tropical Indo-Pacific water inflow into the SCS. At present the SCS has seven main connections to the surrounding seas and oceans (Figure 1). From north to south these are the Taiwan and Bashi Straits (sill depths ~70 and 2500 m, respectively) to the open Pacific Ocean, the Mindoro (450 m) and Balabac (100 m) Straits to the Sulu Sea, the Malaca Strait (30 m) to the Indian Ocean, and the Gaspar and the Karimata Straits (40-50 m) to the Java Sea [*Wyrtki*, 1961]. Thus it is evident that during glacial low sea level, which reached up to ~120 m below the present sea level during LGM [*Fairbanks*, 1989], the SCS was transformed into a semienclosed system connected to the Pacific Ocean only through Bashi Strait and to the Sulu Sea through Mindoro Strait.

The sudden increase in the north-south SST gradient observed in our records at the 5e/5d boundary could be coincident with the shut off of the southern connections to the warm waters of the tropical Indo-Pacific and Java Seas. The reverse process could have occured at Termination I, with the opening of the same channels. In this sense, as shown in the sea level curves of *Chappell and Shackleton* [1986] and *Linsley* [1996], the sea level dropped more than 50 m at the 5e/5d boundary, which is enough to close the southern connections. Accordingly, the southern connections of the SCS to the tropical Indo-Pacific probably remained closed until Termination 1.

A close-up of the four SST profiles for the past 30 kyr is represented in Figure 4. The temperature changes are very similar in all cores, with an approximate temperature rise from the LGM to the present of 2.6°-2.8°C in the south and of ~4°-5°C in the north. As described above, the higher temperature difference in the north probably reflects the different hydrographic conditions due to cut-off of the tropical Indo-Pacific water influx over the Sunda Shelf. Furthermore, glacial times were also characterized by the southward displacement of surface water masses in the open western Pacific [*Thompson*, 1981]. Accordingly, temperate waters that are now situated at 25°-30°N could reach as far south as 20°N, the latitude of the Bashi Strait [*Wang and Wang*, 1990]. As a result of these two processes, the U^{K}_{37}-SST difference between LGM and present in the SCS is larger than the U^{K}_{37}-SST differences observed at other sites at the same latitudes: for example, eastern equatorial Pacific, 1.3°C [*Prahl et al.*, 1989]; central equatorial Atlantic, 1.8°C [*Sikes and Keigwin*, 1994]; and western tropical Pacific, 1.5°C [*Ohkouchi et al.*, 1994].

SST measurements based on foraminiferal studies are also consistent with an amplification of the glacial/interglacial differences in the SCS. Thus temperature increases of 5°-7°C [*Miao et al.*, 1994] in the southern SCS and 6.8°-9.3°C [*Wang and Wang*, 1990] in the northern SCS have been reported for cold season temperatures on the basis of foraminiferal faunal changes. The reported summer increases for the LGM to Holocene period are 0.5°-2.0°C [*Miao et al.*, 1994] and 2°-3°C [*Wang and Wang*, 1990] for south and north SCS, respectively. Differences of 2°-4°C have been reported on the basis of U^{K}_{37}-SST measurements during the past 26 kyr [*Huang et al*, 1997a, b] in two records from the northern SCS (Figure 1).

During the LGM, SST in 17954 reached ~1.2°C lower values than in 17940. This difference could be ascribed to short periods of upwelling of subsurface colder waters at this at site [*Wang et al.*, 1998]. Long-chain C_{37} alkenone concentrations increased slightly during this period (C. Pelejero, unpublished data, 1988). However, other tracers are needed to confirm an upwelling episode at this site.

In the high-resolution (up to bidecadal) record of core 17940, $\delta^{18}O$ in *G.ruber* follows the typical North Atlantic Termination I features, with well-defined Bølling-Allerød and Younger Dryas events (Figure 3) [*Wang et al.*, 1998]. The U^{K}_{37}-SST measurements also follow the same "North Atlantic type" pattern, with values of ~24.5°C during the Bølling-Allerød and a later drop to 23.7°C during the Younger Dryas (Figure 4). The latter event, which was originally thought to be restricted to the North Atlantic and high latitudes, has also been identified in deep-sea sediment records from the Sulu Sea [*Linsley and Thunell*, 1990; *Kudrass et al.*, 1991].

Bølling-Allerød and Younger Dryas events are less well defined in the southern part of the SCS, although core 17964 shows a clear SST plateau at the time of the Bølling-Allerød and a temperature decrease of 0.4°C is shown for the Younger Dryas in core 17961. The same trend can also be observed in the more variable record of core 17961. The low amplitude of SST variation of these events in the southern SCS may partly explain why they were not observed in core V35-5 [*Broecker et al.*, 1988], which is located between 17961 and 17964 (Figure 1). Our results from the SCS confirm that both the Bølling-Allerød and Younger Dryas are synchronous worldwide climatic events.

4. Summary and Conclusions

All SST sediment records in the SCS follow a glacial/interglacial pattern, with a north-south difference of 1°C in the interglacials and nearly 2.5°C in most of the glacial stages (3°C in stage 6). These differences define a temperature offset that remains constant even in episodic heating events such as the SST oscillation centered at 85 kyr B.P.

These north-south temperature differences define two distinct climatic regimes for the SCS that roughly correspond to glacial/interglacial periods, with high SST difference for the glacials and low difference for the interglacials. Transition from one pattern to the other seems to have occurred over short time periods, such as at the end of stage 5e and during warming from LGM to Holocene conditions. These changes probably correspond with sea level fluctuations that permitted or prevented surface seawater exchange with the tropical Indo-Pacific waters in the south.

In both in the northern and southern SCS the U^{K}_{37}-SST differences between LGM and Holocene are between 1° and 3°C higher than those observed at the same latitudes in the Atlantic and Pacific Oceans. This temperature contrast is in agreement with other SST estimates based on foraminiferal assemblages and points to an amplification mechanism that increased the glacial/interglacial differences in this marginal sea.

The deglacial $\delta^{18}O$ and SST profiles exhibit well-defined Bølling-Allerød and Younger Dryas events in Termination I, particularly in the north. The Younger Dryas event shows a cooling of 0.4°-0.8°C with respect to the Bølling-Allerød temperatures in the south and north, respectively.

Comparison of Holocene and stage 5e SSTs shows warmer temperatures (1°-1.2°C) in the previous interglacial period. SSTs were remarkably stable during stage 5e, which contrasts with the significant fluctuations in the $\delta^{18}O$ record. The highest temperature observed in stage 7 lies between that of the Holocene and stage 5e.

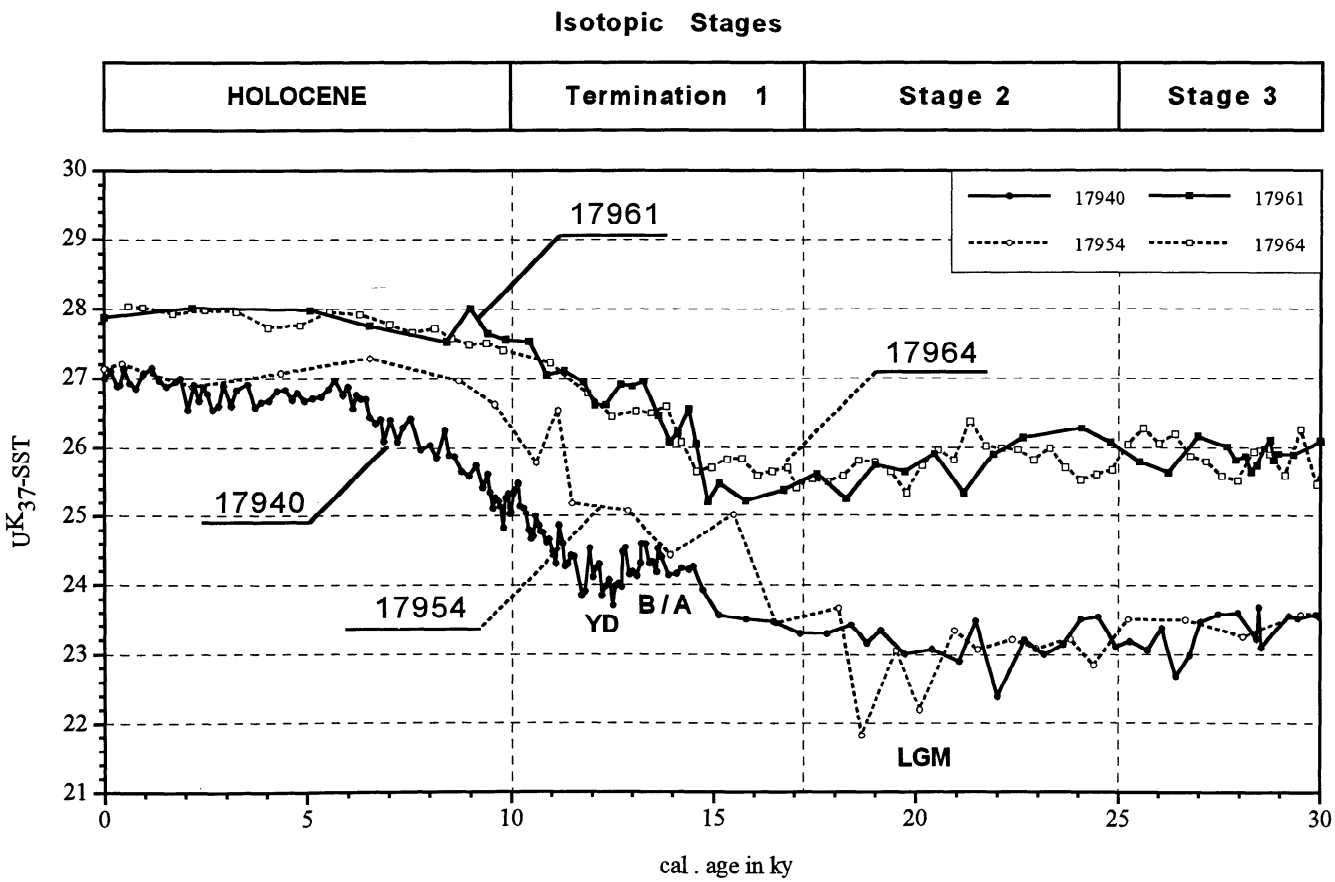

Figure 4. Close-up of the U^{K}_{37}-SST reconstruction for the past 30 kyr. YD is Younger Dryas; B/A is Bølling-Allerød; and LGM is Last Glacial Maximum.

Acknowledgments. Thanks are due to M. Sarnthein for valuable discussions and dedication to South China Sea studies. We sincerely thank S. E. Calvert for comments on an earlier version of this manuscript. CP thanks a Ph.D. grant from C.I.R.I.T. (Generalitat de Catalunya). SH and MK acknowledge funding from the German Academic Exchange Program (DAAD) during the preparation of this manuscript. LW thanks Deutsche Forschungsgemeinschaft for their support in the study. Financial support from the TEMPUS EU project (ENV4-CT97-0564) is acknowledged. The samples included in this study were collected during a R/V Sonne cruise funded by the German Ministry for Education and Research (BMBF). Thanks are also given to D. Anderson, T. Herbert and an anonymous reviewer for their useful comments.

References

Bard, E., B. Hamelin, and R. G. Fairbanks, U-Th ages obtained by mass spectrometry in corals from Barbados: Sea level during the past 130 000 years, *Nature, 346*, 456-458, 1990a.

Bard, E., B. Hamelin, R. G. Fairbanks, and A. Zindler, Calibration of the ^{14}C timescale over the past 30,000 years using mass spectrometric U-Th ages from Barbados corals, *Nature, 345*, 405-410, 1990b.

Bard, E., F. Rostek, and C. Sonzogni, Interhemisphere synchrony of the last deglaciation inferred from alkenone palaeothermometry, *Nature, 385*, 707-710, 1997.

Berger, W.H., Planktonic foraminifera: Selective solution and paleoclimatic interpretation, *Deep Sea Res. Oceanogr. Abstr., 15*, 31-43, 1968.

Brassell, S. C., G. Eglinton, I. T. Marlowe, U. Pflaumann, and M. Sarnthein, Molecular stratigraphy: A new tool for climatic assessment, *Nature, 320*, 129-133, 1986.

Broecker, W. S., M. Andree, M. Klas, G. Bonani, W. Wolfli, and H. Oeschger, New evidence from the South China Sea for an abrupt termination of the last glacial period, *Nature, 333*, 156-158, 1988.

Chappell, J., and N. J. Shackleton, Oxygen isotopes and sea level, *Nature, 324*, 137-140, 1986.

Cornu, S., J. Patzold, E. Bard, J. Meco, and J. Cuerda-Barcelo, Paleotemperature of the last interglacial period based on $\delta^{18}O$ of *Strombus bubonius* from the western Mediterranean Sea, *Paleogeogr. Paleoclimatol. Paleoecol., 103*, 1-20, 1993.

Fairbanks, R.G., A 17,000-year glacio-eustatic sea level record: Influence of glacial melting rates on the Younger Dryas event and deep-ocean circulation, *Nature, 342*, 637-642, 1989.

Grootes, P. M., and M. Stuiver, Oxygen 18/16 variability in Greenland snow and ice with 10^{-3} to 10^{5}-year time resolution, *J. Geophys. Res., 102*, 26,455-26,470, 1997.

Heilig, S., Paläo-Ozeanographie vor Vietnam im Wandel von Glazial zu Interglazial, Unveröffentl. M.Sc. thesis, Christian-Albrechts-Universität, Kiel, Germany, 1996.

Huang, C.-Y., P.-M. Liew, M. Zhao, T.-C. Chang, C.-M. Kuo, M.-T. Chen, C.-H. Wang, and L.-F. Zheng, Deep sea and lake records of the southeast Asian paleomonsoons for the last 25 thousand years, *Earth Planet. Sci. Lett., 146*, 59-72, 1997a.

Huang, C.-Y., S.-F. Wu, M. Zhao, M.-T. Chen, C.-H. Wang, X. Tu, and P.-B. Yuan, Surface ocean and monsoon climate variability in the South China Sea since the last glaciation, *Mar. Micropaleontol., 32*, 71-94, 1997b.

Jian, Z., L. Wang, M. Kienast, M. Sarnthein, W. Kuhnt, H. Lin, and P. Wang, Benthic foraminiferal paleoceanography of the South China Sea over the last 40.000 years, *Mar. Geol.*, in press,1998.

Kienast, M., Geschichte des Fluvialeintrags vom Sunda-Schelf: Abbild in hemipelagischen Sedimenten aus dem Südchinesischen Meer. M.Sc. thesis, pp. 1-53, Kiel University, Kiel, Germany, 1996.

Kudrass, H. R., H. Erlenkeuser, R. Vollbrecht, and W. Weiss, Global nature of the Younger Dryas cooling event inferred from oxygen isotope data from Sulu Sea cores, *Nature, 349*, 406-409, 1991.

Levitus, S., *World Ocean Atlas.* U.S. Gov. Print. Off. Washington, D.C., 1994.

Linsley, B. K., Oxygen-isotope record of sea level and climate variations in the Sulu Sea over the past 150,000 years, *Nature, 380*, 234-237, 1996.

Linsley, B. K., and R. C. Thunell, The record of deglaciation in the Sulu Sea: Evidence for the Younger Dryas event in the tropical western Pacific, *Paleoceanography, 5*, 1025-1039, 1990.

Madureira, L. A. S., M. H. Conte, and G. Eglinton, Early diagenesis of lipid biomarker compounds in North Atlantic sediments, *Paleoceanography, 10*, 627-642, 1995.

Martinson, D. G., N. G. Pisias, J. D. Hays, J. J Imbrie, T. C. Moore, and N. J. Shackleton, Age dating and the orbital theory of the ice ages: Development of a high-resolution 0 to 300,000 year chronostratigraphy, *Quat. Res., 27*, 1-29, 1987.

McCaffrey, M.A., J.W. Farrington, and D.J. Repeta, The organic geochemistry of Peru margin surface sediments: I. A comparison of the C_{37} alkenone and historical El Nino record, *Geochim. Cosmochim. Acta, 54*, 1671-1682, 1990.

Miao, Q., R. C. Thunell, and D. M. Anderson, Glacial-Holocene carbonate dissolution and sea surface temperatures in the South China and Sulu Seas, *Paleoceanography, 9*, 269-290, 1994.

Molengraaff, G. A. F., Modern deep-sea research in the East Indian Archipelago, *Geogr. J. 57*, 95-121, 1921.

Müller, P. J., G. Kirst, G. Ruhland, I. von Storch, and A. Rosell-Melé, Calibration of the alkenone paleotemperature index $U^{K'}_{37}$ based on core-tops from the eastern South Atlantic and the global ocean (60°N-60°S), *Geochim. Cosmochim. Acta, 62*, 1757-1772, 1998.

Ohkouchi, N., K. Kawamura, T. Nakamura, and A. Taira, Small changes in the sea surface temperature during the last 20,000 years: Molecular evidence from the western tropical Pacific, *Geophys. Res. Lett., 21*, 2207-2210, 1994.

Pelejero, C., and J. O. Grimalt, The correlation between the U^{K}_{37} index and sea surface temperatures in the warm boundary: The South China Sea, *Geochim. Cosmochim. Acta, 61*, 4789-4797, 1997.

Prahl, F. G., and S. G. Wakeham, Calibration of unsaturation patterns in long-chain ketone compositions for palaeotemperature assessment, *Nature, 330*, 367-369, 1987.

Prahl, F. G., L. A. Muehlhausen, and M. Lyle, An organic geochemical assessment of oceanographic conditions at MANOP Site C over the past 26,000 years, *Paleoceanography, 4*, 495-510, 1989.

Prahl, F. G., R. B. Collier, J. Dymond, M. Lyle, and M.A. Sparrow, A biomarker perspective on Prymnesiophyte productivity in the northeast Pacific Ocean, *Deep Sea Res. I, 40*, 2061-2076, 1993.

Rostek, F., G. Ruhland, F. C. Bassinot, P. J. Müller, L. D. Labeyrie, Y. Lancelot, and E. Bard, Reconstructing sea surface temperature and salinity using $\delta^{18}O$ and alkenone records, *Nature, 364*, 319-321, 1993.

Sarnthein, M., U. Pflaumann, P. X. Wang, and H. K. Wong, Preliminary report of the Sonne-95 cruise "Monitor Monsoon" to the South China Sea" *Berichte Rep. 68*, Geol.-Paläontol. Inst., Univ. of Kiel, Kiel, Germany, 1994.

Schneider, R. R., P. J. Müller, and G. Ruhland, Late Quaternary surface circulation in the east equatorial South Atlantic: Evidence from alkenone sea surface temperatures, *Paleoceanography, 10*, 197-219, 1995.

Schönfeld, J., and H. R. Kudrass, Hemipelagic sediment accumulation rates in the South China Sea related to late Quaternary sea-level changes, *Quat. Res., 40*, 368-379, 1993.

Sikes, E. L., and L. Keigwin, Equatorial Atlantic sea surface temperature for the last 30 kyr: A comparison of $U^{K'}_{37}$, $\delta^{18}O$, and foraminiferal assemblage temperature estimates, *Paleoceanography, 9*, 31-45, 1994.

Sikes, E. L., J. W. Farrington, and L. D. Keigwin, Use of the alkenone unsaturation ratio U^{K}_{37} to determine past sea surface temperatures: Core-top SST calibrations and methodology considerations, *Earth Planet. Sci. Lett., 104*, 36-47, 1991.

Stuiver, M., and T. F. Braziunas, Modeling atmospheric ^{14}C influences and ^{14}C ages of marine samples to 10,000 BC, *Radiocarbon, 35*, 137-189, 1993.

Summerhayes, C. P., D. Kroon, A. Rosell-Mele, R. W. Jordan, H.-J. Schrader, R. Hearn, J. Villanueva, J. O. Grimalt, and G. Eglinton, Variability in the Benguela Current upwelling system over the past 70,000 years, *Prog. Oceanogr., 35*, 207-251, 1995.

Thompson, P., Planktonic foraminifera in the western North Pacific during the past 150,000

years: Comparison of modern and fossil assemblages, *Palaeogeogr. Palaeoclimatol. Palaeoecol., 35*, 241-279, 1981.

Villanueva, J., C. Pelejero, and J. O. Grimalt, Clean-up procedures for the unbiassed estimation of C_{37}-C_{39} alkenones sea surface temperatures and terrigenous *n*-alkane inputs in paleoceanography, *J. Chromatogr. A, 757*, 145-151, 1997.

Villanueva, J., J. O. Grimalt, E. Cortijo, L. Vidal, and L. Labeyrie, Assessment of sea surface temperature variations in the central North Atlantic using the alkenone unsaturation index ($U^{K'}_{37}$), *Geochim. Cosmochim. Acta, 62*, 2421-2427, 1998.

Wang, L., and P. Wang, Late Quaternary paleoceanography of the South China Sea: Glacial-interglacial contrasts in an enclosed basin, *Paleoceanography, 5*, 77-90, 1990.

Wang, L., M. Sarnthein, H. Erlenkeuser, J. O. Grimalt, P. Grootes, S. Heilig, E. Ivanova, M. Kienast, C. Pelejero, and U. Pflaumann, East Asian monsoon climate during the late Pleistocene: High-resolution sediment records from the South China Sea, *Mar. Geol.*, in press, 1998.

Wyrtki, K., Physical oceanography of the southeast Asian waters. *Scientific results of marine investigations of the South China Sea and the Gulf of Thailand,* Report 1961, vol. 2. , NAGA, Scripps Inst., Oceanography, La Jolla, Calif., 1961.

Zhao, M., A. Rosell, and G. Eglinton, Comparison of two U^{k}_{37}-sea surface temperature records for the last climatic cycle at ODP Site 658 from the subtropical Northeast Atlantic, *Palaeogeogr. Palaeoclimatol. Palaeoecol., 103*, 57-65, 1993.

J.O. Grimalt and C. Pelejero, Department of Environmental Chemistry (ICER-CSIC), Jordi Girona, 18, 08034 Barcelona, Catalonia, Spain. (e-mail: jgoqam@cid.csic.es; cpbqam@cid.csic.es)

S. Heilig and M. Kienast, Department of Geosicence, University of British Columbia, Vancouver, B.C., Canada V6T 1Z4. (e-mail: heilig@unixg.ubc.ca; kienast@unixg.ubc.ca)

L. Wang, Department of Geoscience, Graduate School of Environmental Earth Science, Hokkaido University, Sapporo, 060-0810 Japan. (ljwang@ees.hokudai.ac.jp)

(Received July 9, 1998;
revised October 28, 1998;
accepted November 1, 1998.)